

Synthesis Rare Earth Oxide and Its Effect of Process Temperature on Compound Composition

Fitria Hidayanti

Physics Engineering Department, Universitas Nasional
Jalan Sawo Manila No. 61, Pejaten, Pasar Minggu, Jakarta 12520, Indonesia
Email: fitriahidayanti@gmail.com

Received: 22nd December 2019, Accepted: 22nd January 2020, Published: 29th February 2020

Abstract

Rare earth oxide (La_2O_3) has been synthesized using $\text{La}(\text{NO}_3)_3 \cdot 6\text{H}_2\text{O}$ as precursor solution. 1 mmol Lanthanum Nitrate Hexahydrate ($\text{La}(\text{NO}_3)_3 \cdot 6\text{H}_2\text{O}$), 5 mmol Nickel Nitrate Hexahydrate ($\text{Ni}(\text{NO}_3)_2 \cdot 6\text{H}_2\text{O}$) and 7.2 mmol Glycine ($\text{C}_2\text{H}_5\text{NO}_2$) proceed by solution combustion synthesis methods. An analysis of X-Ray Diffraction was conducted for lanthanum oxide phase and compound composition on different process temperature. Lanthanum oxide (La_2O_3) phase appears at 2θ angle between 10° up to 90° with process temperature at room temperature, 60°C , 70°C and 80°C .

Keywords

Rare Earth, La_2O_3 , X-ray Diffraction, Compound Composition.

Introduction

Lanthanum oxide (La_2O_3) as rare earth oxide has a great of incredible and excellent properties that allowable its broad application in technological and industrial such as piezoelectric materials to increase piezoelectric product coefficient [1], optical filters [2], optical fiber [1], optical glass [1], support for metal [2], improve the burning rate of propellant [1], catalyst [4, 5], electrode material [1], light-emitting material (blue powder) [1], as regard higher photoelectric conversion efficiency [1], light-converting agricultural film [1], hydrogen storage material [1], laser material [1], and dielectric material [6, 7].

In this work, lanthanum oxide synthesized by a method of solution combustion synthesis (SCS), an application process for synthesis a material in nanoscale, versatile and efficient in the use of energy that has been used in the production of various type of ceramics powder for several types of advanced application.

The SCS method is an unsophisticated method, but an essential way in the synthesis nanostructures of oxide, metal, spinel, alloy, and intermetallic [8]. This method is based on the exothermic process between nitrate (oxidizing agent) and organic substances (reducing agents) by directly producing nanostructured powder [8, 9].

Utilization of exothermic reaction as a source to drive the reaction itself, so that no external source is needed and only requires ignition temperature to start the process. Crucial advantages of SCS method are (1) mixing of the initial reaction that occurs in the liquid state thereby enabling control of the composition, structure, stoichiometry of reaction product and homogeneity, (2) probability of incorporating impurity dopant ions in the form of oxides, to prepare materials that are suitable for industrial needs, (3) the fastest SCS method allows the formation of metastable phase [8, 10, 11].

In this research, lanthanum oxide (La_2O_3) was synthesized at room temperature, 60°C , 70°C and 80°C and characterized by XRD.

Materials and Methods

Synthesis of Rare Earth Oxide (La_2O_3)

The precursors used in this synthesis process include 0.433 grams (1 mmol) Lanthanum Nitrate Hexahydrate ($\text{La}(\text{NO}_3)_3 \cdot 6\text{H}_2\text{O}$) by Merck, 1.454 grams (5 mmol) Nickel Nitrate Hexahydrate ($\text{Ni}(\text{NO}_3)_2 \cdot 6\text{H}_2\text{O}$) by Merck, and 0.976 grams (7.2 mmol) Glycine ($\text{C}_2\text{H}_5\text{NO}_2$) by Merck. Then, the precursors dissolved in 10 mL aqua dm and simultaneously stirring using magnetic stirring with a total mass of 12.863 grams.

The temperature variations carried out in the stirring process at temperatures 60°C , 70°C and 80°C . When the stirring process reaches the desired temperature, the temperature of the solution is stabilized at a set point 60°C , 70°C , and 80°C . The transparent green solution result of stirring process on the beaker glass is transferred into the cup for further drying process which aims to remove water. This drying process is carried out for 3 hours and 20 minutes until the gel is formed.

The gel obtained from the drying process was calcined at high temperatures under the melting point. In addition, this process aims to eliminate volatile elements and form La_2O_3 . The gel was calcinated at temperature 500°C to produce oxide with a heat rate of $10^\circ\text{C}/\text{min}$ and then held for two hours. Having the gel reaches ignition temperature, combustion occurred and changes it into a sponge shape with volume development. The expanded sample mashed using a mortar to obtain a powder sample.

Characterization Technique

Characterization technique was conducted by x-ray diffraction, XRD SmartLab Rigaku. XRD characterization was conducted under test conditions with a current of 30 mA and a voltage of 40 kV. The target element used to radiate the sample is Cu K α with wavelength specifications 1.5406 Å. Besides the STEP mode scan with a scan speed of 0.25 and a scan range of 10⁰ - 90⁰ 2 θ for each sample. Then an analysis of the diffraction pattern of the black powder sample was conducted using the Rietveld method using Panalytical High Score Plus software. The flow chart of research shown in Figure 1.

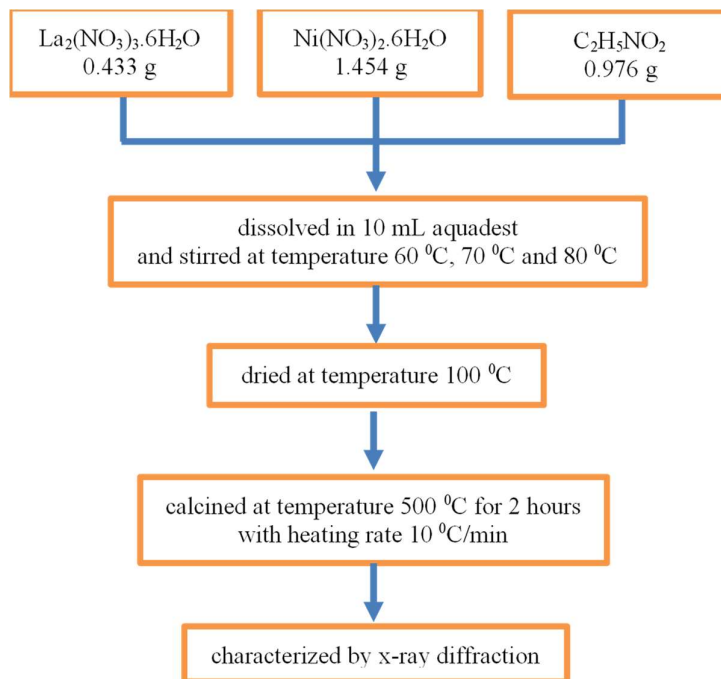


Figure 1: Flowchart Synthesis and Characterization of La₂O₃

Results and Discussion

The diffraction pattern of the sample with a variety of synthesis temperature at 60 °C, 70 °C, and 80 °C shown in Figure 2. It is known that in the angular range of 10⁰ - 90⁰, there is an identical diffraction peak pattern of powder samples, the identical peak pattern in the 2 θ angles, including 37⁰, 43⁰, 62⁰, 75⁰ and 79⁰ which are identified as phase of nickel oxide.

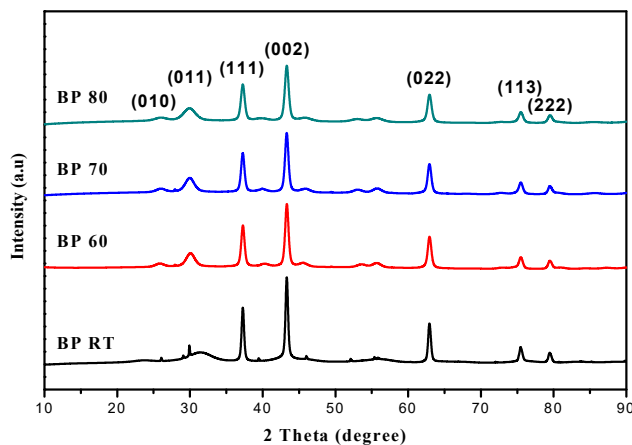


Figure 2: Diffraction Peaks Pattern of the Powder Sample

Meanwhile, Figure 3 is a magnification of diffraction peaks in Figure 2 with 2θ angle range of 20° to 40° . In the black powder sample at room temperature can be indicated at 2θ angle of 26° , 29° , 30° , and 31° are the peaks of the lanthanum oxide (La_2O_3) phase. While at 2θ angle of 23° and 31° is the phase of the lanthanum nickel tetraoxide (La_2NiO_4).

In addition, it was also observed at the diffractogram peaks for black powder sample at 60°C , 70°C , and 80°C . There is an identical peak seen at 2θ angle of 25° and 30° , which is the phase of lanthanum oxide (La_2O_3). While for the peak at 2θ angle of 28° , shrinkage occurs as temperature synthesis rises, which indicates the lanthanum oxide Ht (x-form) phase.

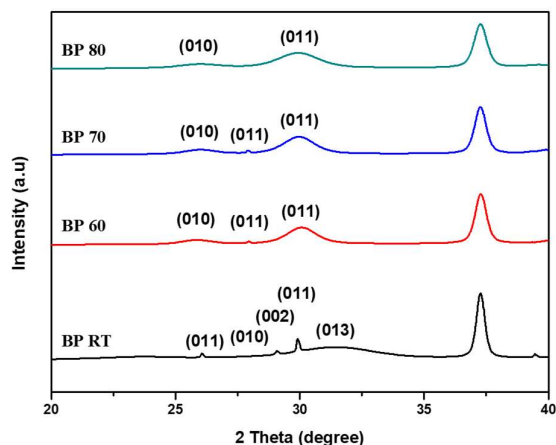


Figure 3: La_2O_3 Diffraction Pattern at 2θ angle $20^\circ - 40^\circ$

In Figure 4 there are formations of peaks in the range of 30° to 60° . Peaks at 39° and 44° show the lanthanum oxide (La_2O_3) phase as increasing synthesis temperature as well as increasing formation of the peak. It shows more clearly that the lanthanum oxide phase is formed. Similarly, around angle 40° and 45° appear a diffractogram peak that showed the development of the phase of lanthanum nickel trioxide at room temperature, but along the increase in temperature appeared lanthanum oxide (La_2O_3) phase at the peak at 53° and 55° .

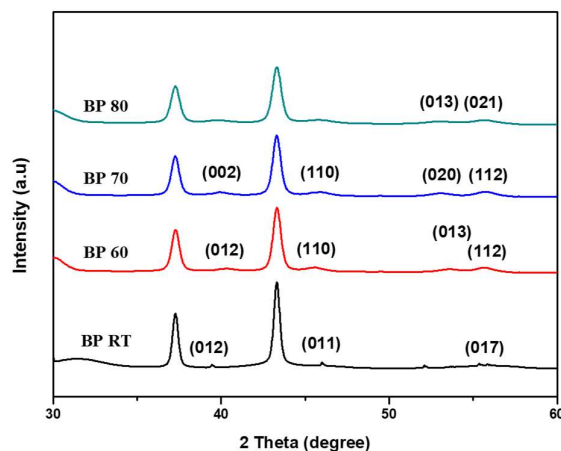


Figure 4: La_2O_3 Diffraction Pattern at 2θ angle $30^\circ - 60^\circ$

An evaluating from suitable criteria for the profile fitting process based on the literature, the excellent refinement match is determined by the weighted-profile R-index (R_{wp}) and goodness of fit (GoF) parameters. R_{wp} is a weight comparison pattern of the difference between observation patterns with XRD calculations [12].

The ideal value of R_{wp} is $<10\%$ [12, 13]. While $R_{expected}$ is a statistical evaluation of noise data on diffractograms. In addition, the parameter of the goodness of fit (GoF) or commonly known as Chi-Squared is a ratio of XRD observation patterns that are comparable with expected, with an ideal value of no more than 4% [13]. The goodness of fit and R_{wp} factors and size of the crystallite that have been calculated using High Score Plus for each black powder sample are known respectively in Table 1.

Table 1: Match Parameter and Crystallite Size of Samples

Sample	Parameter			Crystallite Size (nm)
	R _{expected}	R _{wp}	GoF	
Black powder Room Temperature (RT)	9.1453	7.9019	1.1902	2.0737
Black powder 60 °C	9.0551	8.1407	1.2738	5.0808
Black powder 70 °C	9.1597	8.1181	1.2420	4.3323
Black powder 80 °C	8.9618	7.6367	1.1468	3.4879

From Table 1, it can be concluded that goodness of fit for each black powder sample can be categorized very well. The analysis result of compounds composition contained in each black powder sample is listed in Table 2. Table 2 shows that lanthanum oxide (La₂O₃) phase formed on room temperature, 60 °C, 70 °C and 80 °C with a composition of 1.3%, 15.3%, 17.8% and 19.3%, respectively.

Table 2: Compound Composition of Phases

Compound	Compound Composition (%)			
	RT	60 °C	70 °C	80 °C
La ₂ NiO ₄	27.4	-	-	-
NiO	71.3	84.6	82.0	80.7
La ₂ O ₃	1.3	15.3	17.8	19.3
La ₂ O ₃ – Ht (x-form)	-	0.1	0.2	-
Total of phase composition	100	100	100	100

Table 2 shows that the synthesis temperature directly proportional to La₂O₃ phase composition. Increasing of lanthanum oxide phase due to oxidation at higher temperature quickly occurred.

Conclusions

In this study, lanthanum oxide (La₂O₃) as rare earth oxide successfully formed with a variety synthesis temperature at room temperature, 60 °C, 70 °C, and 80 °C with the Solution Combustion Synthesis (SCS) method. Analysis results of x-ray diffraction (XRD) from each sample indicated that beside lanthanum oxide (La₂O₃) there were several phases contained in the black powder, i.e. Lanthanum Oxide Ht (x-form), Lanthanum Nickel Oxide (La₂NiO₄), and Nickel Oxide (NiO). By varying synthesis temperature, the composition of the Lanthanum Oxide (La₂O₃) phase increase on temperature process. Lanthanum oxide (La₂O₃) phase formed on room temperature, 60 °C, 70 °C and 80 °C with a composition of 1.3%, 15.3%, 17.8% and 19.3%, respectively.

References

1. Saravani, H. and M. Khajehali, Synthesis and characterization of lanthanum oxide and lanthanum oxide carbonate nanoparticles from thermolysis of [La (acac)(NO₃)(H₂O)] complex. *Oriental Journal of Chemistry*, 2015. 31(4): p. 2351.
2. Rieck, J.S. and A.T. Bell, Studies of the interactions of H₂ and CO with PdSiO₂ promoted with La₂O₃, CeO₂, Pr₆O₁₁, Nd₂O₃, and Sm₂O₃. *Journal of catalysis*, 1986. 99(2): p. 278-292.
3. Saravani, H. and M. Jehali, Synthesis and Characterization of Lanthanum Oxide and Lanthanum oxide Carbonate Nanoparticles from Thermalizes of [La (acac)(NO₃)(H₂O)]. *Oriental Journal of Chemistry*, 2015. 32(1): p. 491-498.
4. Rosynek, M.P. and D.T. Magnuson, Preparation and characterization of catalytic lanthanum oxide. *Journal of Catalysis*, 1977. 46(3): p. 402-413.
5. Ghiasi, M. and A. Malekzadeh, Synthesis, characterization and photocatalytic properties of lanthanum oxy-carbonate, lanthanum oxide and lanthanum hydroxide nanoparticles. *Superlattices and Microstructures*, 2015. 77: p. 295-304.
6. Zhao, Y., Design of higher-k and more stable rare earth oxides as gate dielectrics for advanced CMOS devices. *Materials*, 2012. 5(8): p. 1413-1438.
7. Wong, H., et al., The interfaces of lanthanum oxide-based subnanometer EOT gate dielectrics. *Nanoscale research letters*, 2014. 9(1): p. 472.
8. Xanthopoulou, G., et al., Solution combustion synthesis of nano-catalysts with a hierarchical structure. *Journal of catalysis*, 2018. 364: p. 112-124.
9. Deganello, F. and A.K. Tyagi, Solution combustion synthesis, energy and environment: Best parameters for better materials. *Progress in Crystal Growth and Characterization of Materials*, 2018. 64(2): p. 23-61.

10. Ozer, D., et al., Fuel effects on $\text{Li}_2\text{CuP}_2\text{O}_7$ synthesized by solution combustion method for lithium-ion batteries. *Ceramics International*, 2019. 45(4): p. 4626-4630.
11. Manukyan, K.V., Template-Assisted Solution Combustion Synthesis, in *Concise Encyclopedia of Self-Propagating High-Temperature Synthesis*. 2017, Elsevier. p. 376-378.
12. Speakman, S.A., Profile Fitting for Analysis of XRPD Data using HighScore Plus v3. Massachusetts Institute of Technology, Cambridge MA, 2012.
13. Sarwanto, Y. and W.A. Adi, Crystallographic Structure and Magnetic Properties of Pseudobrookite $\text{Fe}_{2-x}\text{Ni}_x\text{TiO}_5$ System ($X=0, 0.1, 0.2, 0.3, 0.5$ and 1). *Jusami| Indonesian Journal of Materials Science*, 2018. 19(2): p. 47-53.